Neuroretinal Cell Death in a Murine Model of Closed Globe Injury: Pathological and Functional Characterization

Richard J. Blanch,[1,2] *Zubair Ahmed,*[1] *Attila Sik,*[1] *David R. J. Snead,*[3] *Peter A. Good,*[4] *Jenna O'Neill,*[1] *Martin Berry,*[1] *Robert A. H. Scott,*[2,4,5] *and Ann Logan*[1,5]

Purpose. Blunt ocular trauma causes severe retinal injury with death of neuroretinal tissue, scarring, and permanent visual loss. The mechanisms of cell death are not known, and there are no therapeutic interventions that improve visual outcome. We aimed to study the extent, distribution, and functional consequences of cell death by developing and characterizing a rat model of retinal injury caused by blunt ocular trauma.

Methods. The eyes of anesthetized adult rats were injured by either weight drop or low-velocity ballistic trauma and assessed by clinical examination, electroretinography, light microscopy, electron microscopy, and TUNEL. Projectile velocity was measured and standardized.

Results. Weight drop did not cause reproducible retinal injury, and the energy threshold for retinal injury was similar to that for rupture. Low-velocity ballistic trauma to the inferior sclera created a reproducible retinal injury, with central sclopetaria retinae, retinal necrosis, and surrounding commotio retinae with specific photoreceptor cell death and sparing of cells in the other retinal layers. The extent of photoreceptor cell death declined and necrosis progressed to apoptosis with increasing distance from the impact site.

Conclusions. This is the only murine model of closed globe injury and the only model of retinal trauma with specific photoreceptor cell death. The clinical appearance mirrors that in severe retinal injury after blunt ocular trauma in humans, and the ultrastructural features are consistent with human and animal studies of commotio retinae. After ocular trauma, photoreceptor apoptosis may be prevented and visual outcomes improved by blocking of the cell death pathways. (*Invest Ophthalmol Vis Sci.* 2012;53:7220–7226) DOI: 10.1167/iovs.12-9887

From the [1]Neurotrauma and Neurodegeneration Section, Clinical and Experimental Medicine, University of Birmingham, Birmingham, United Kingdom; the [2]Academic Department of Military Surgery and Trauma, Royal Centre for Defence Medicine, Birmingham, United Kingdom; the [3]University Hospitals Coventry and Warwickshire NHS Trust, Coventry, United Kingdom; and the [4]Birmingham and Midland Eye Centre, Birmingham, United Kingdom.

[5]These authors are joint senior authors.

Supported by the Ministry of Defence, United Kingdom; the Drummond Foundation, United Kingdom; and the Sir Ian Fraser Foundation, Blind Veterans UK.

Submitted for publication March 20, 2012; revised July 28, 2012; accepted September 11, 2012.

Disclosure: **R.J. Blanch**, None; **Z. Ahmed**, None; **A. Sik**, None; **D.R.J. Snead**, None; **P.A. Good**, None; **J. O'Neill**, None; **M. Berry**, None; **R.A.H. Scott**, None; **A. Logan**, None

Corresponding author: Richard J. Blanch, Molecular Neuroscience Research Group, IBR West (2nd Floor), Medical School, University of Birmingham, Edgbaston, Birmingham B15 2TT, United Kingdom; rjb017@bham.ac.uk.

Ocular trauma affects 20% of Americans during their lifetime, and 0.6% to 1% of these suffer retinal injury.[1–3] Personnel in war zones are at much higher risk, and up to 13% of soldiers wounded in action sustain an ocular injury, of whom 50% to 60% have retinal injuries.[4,5] Retinal trauma occurs with penetrating and perforating globe injuries, ruptures, and contusion-type closed globe injuries including those caused by blast.[6,7]

Retinal injury caused by blunt trauma is characterized clinically as commotio retinae (Berlin's edema) or the more severe sclopetaria retinae.[8,9] Commotio retinae describes gray-white opacification of the neuroretina caused by blunt ocular trauma and covers a spectrum of injury from self-limiting to severe with permanent visual loss.[10,11] Commotio retinae has been modeled in pigs, rabbits, cats, and rhesus and owl monkeys, demonstrating traumatic disruption of the photoreceptor outer segments,[12–14] which is also seen on optical coherence tomography (OCT) and fundus reflection densitometry in humans.[11,15] The outer segments are phagocytosed by retinal pigment epithelium (RPE) cells. The RPE becomes a multilayered disorganized structure, sometimes directly opposed to the inner segments.[14] Though photoreceptor cell death has been noted in animal models, the focus of previous studies was disruption and subsequent recovery of photoreceptor outer segments; the extent, distribution, and type of cell death have not been reported.[14,16] After severe blunt ocular trauma in humans, commotio retinae features disruption of the inner–outer segment junction and progresses to outer retinal atrophy with degeneration of photoreceptors.[17]

Rats are an ideal species in which to model ocular trauma due to the similarities of their retina with that of humans, the ready availability of antibodies for immunohistochemical studies, the low capital costs, and the ease of husbandry and surgical interventions.[12] Previous animal studies of commotio retinae used modified air guns or a catapult to deliver high-velocity (20-50 m/s) projectiles to the eye,[12] but such methods cannot precisely control and calibrate the energy delivered. For the pig, 0.49 J is sufficient to cause commotio retinae, and thus we hypothesized that a lower energy would be required in the smaller, more delicate rat eye.[12]

We report a rat model of retinal injury induced by low-energy blunt ocular trauma, which features commotio retinae and sclopetaria retinae with specific photoreceptor cell death. This correlates well with reported loss of the outer nuclear layer (ONL) observed by OCT in patients with long-term visual loss after commotio retinae.[17]

Materials and Methods

Animal Care and Procedures

Animal procedures were evaluated and licensed by the UK Home Office, approved by the University of Birmingham's Biomedical Ethics Review Sub-Committee, and conducted in accordance with the ARVO Statement

Investigative Ophthalmology & Visual Science, October 2012, Vol. 53, No. 11

for the Use of Animals in Ophthalmic and Vision Research. Female rats weighing 170 to 200 g were purchased from Charles River Laboratories (Margate, UK), kept on a 12-hour light/dark cycle with a daytime luminance of 80 lux, and fed and watered ad libitum (as in all our previous studies of central nervous system injury[18]). Wistar rats were used for studies of weight drop and Lister hooded rats for studies of ballistic injury, except where otherwise stated. All injuries were induced under general anesthesia with inhaled isofluorane in oxygen. For electron microscopy (EM) and terminal deoxynucleotidyl transferase-mediated dUTP nick-end labeling (TUNEL), animals were killed by perfusion with fixative under terminal anesthesia with intraperitoneal ketamine/medetomidine. Electroretinograms (ERG) were recorded under general anesthesia with intraperitoneal ketamine/medetomidine, and animals were killed by intraperitoneal overdose of pentobarbitone for retinal whole mounts.

Weight Drop Injury

Weights were dropped from a height of 50 cm onto the lateral sclera. Six groups of rats were injured by weight drop (2–6 eyes of 2–4 rats per group). Weights of 22.6 g (0.111 J) and 31.3 g (0.154 J) with 6 mm flat tips were dropped onto the central cornea, and rats were killed at 2 hours after injury. Weights of 17.6 g (0.086 J) and 23.0 g (0.113 J) with 3 mm flat tips and 22.6 and 31.3 g with 6 mm flat tips were dropped onto the lateral sclera, and animals were killed at 2 days after injury. To increase the energy of the weight drop method, a 7 cm doubled section of catapult latex (Match System superpower catapult latex; Middy Tackle International, Heanor, UK), stretched by 7 cm, was used to propel a 22.6 g/6 mm tip weight downward; animals were killed at 2 days after injury. Additional Lister hooded rats were injured with a 31.3 g weight/6 mm tip plus catapult latex. The catapult latex gave a measured impact energy of 0.6 J for both 22.6 and 31.3 g weights due to inefficiencies in the system. Velocity was calculated for weight drop as gravitational potential energy; the additional energy of the catapult latex was calculated by distance traveled when fired horizontally from a known height.

Ballistic Injury

Injury was created by firing a dome-headed (air gun pellet) or spherical (ball bearing) weight down a 5.5 × 300 mm steel barrel using compressed air held in a 500 mL reservoir with pressure monitoring, released by a solenoid-actuated valve (response time <5 ms, flow coefficient [Cv] 491 NL/min; SMC Pneumatics, Milton Keynes, UK). Projectiles were plastic ball bearings (0.095 g), plastic 0.22-caliber pellets (0.5 g), and metal 0.22-caliber air gun pellets (0.91 g). Projectile velocity was measured using a PC sound card.[19] Briefly, a Dell Studio XPS (Dell Corporation Ltd., Berkshire, UK) laptop was used to record the sound of the compressed air device being fired using MAGIX Music Editor 3 (MAGIX AG, Reno, NV) at a metal plate at known distance from the muzzle. The resultant waveform was then viewed and the time between air first leaving the barrel and the impact with the metal plate recorded at 1, 10.5, 22, 31.5, and 42 cm for 10 iterations at each distance. Mean velocity was calculated at the different time points.

Wistar rats ($n = 13$ rats, 26 eyes) were used for cadaveric studies to determine the risk of rupture. Female Lister hooded rats were used to study the effects of a 0.095 g projectile delivered at 20 m/s to the sclera: (1) bilaterally for EM studies before killing at 2 hours (lateral scleral impact; $n = 4$ animals), 2 days (inferior scleral impact; $n = 4$ animals), and 14 days (inferior scleral impact; $n = 4$ animals) after injury; (2) unilaterally to inferior sclera for TUNEL and immunohistochemical studies before killing at 2 days ($n = 4$ animals); and (3) unilaterally to inferior sclera for ERG studies and retinal whole mounts before killing at 2 weeks ($n = 8$ animals).

In Vivo Imaging

Animals were examined immediately after injury, at 2 days, and at 14 days by indirect ophthalmoscopy.

Electroretinography

ERG were recorded (HMsERG; Ocuscience, Kansas City, MO) at 2, 7, and 14 days after ballistic injury and interpreted using ERGView (Ocuscience). Animals were dark adapted overnight and prepared for ERG under dim red light (>630 nm). Scotopic flash ERG were recorded at −2.5, 0, and +0.5 log units with respect to standard flash and photopic flash ERG with background illumination of 30,000 mcd/m^2 at 0 and +0.5 log units, using DTL fiber (Unimed Electrode Supplies, Farnham, UK) corneal electrodes with pressure-molded Aclar (Agar Scientific, Stansted, UK) contact lenses and needle skin electrodes (Unimed).

Electron Microscopy

The primary tissue fixative was 4% gluteraldehyde in 0.1 M phosphate buffer (PB; pH 7.3) as used in previous studies of commotio retinae.[13,14] Eyes were removed and the cornea incised before 24 hours postfixation in the primary fixative at room temperature. A section of injured retina was dissected out, washed in 0.1 M PB, postfixed in 1% osmium tetroxide in 0.1 M PB for 45 minutes, washed in PB, dehydrated in ascending concentrations of ethanol, and immersed in propylene oxide before infiltrating in resin (Durcupan; Electron Microscopy Sciences, Hatfield, PA) for 24 hours and polymerizing at 56°C for 24 hours. Semithin sections (1 μm thick) were cut using glass knives on an "ultracut" ultramicrotome (Reichert-Jung, Vienna, Austria). Sections were stained with toludine blue. Ultrathin gold sections (70–90 nm) were cut with a glass or diamond knife, floated on distilled water, mounted on formvar-coated 50-mesh copper grids, stained with uranyl acetate and lead citrate, and examined on a JEOL 1200 EX transmission electron microscope (JEOL [UK] Ltd., Welwyn Garden City, UK) fitted with a LaB6 filament at an operating voltage of 80 keV.

TUNEL and Immunohistochemistry

The tissue fixative was 4% paraformaldehyde (PFA) in phosphate-buffered saline. Eyes were removed, and the cornea was incised before 24 hours postfixation at 4°C. Specimens were cryoprotected in ascending concentrations of sucrose in phosphate-buffered saline (PBS) at 4°C; the anterior segments were removed, and the retinal cup was embedded in OCT and stored at −80°C. Sections 15 μm thick were cut using a cryostat (Bright Instruments, Huntingdon, UK) and adhered onto SuperfrostTM (Fisher, Loughborough, UK)-coated glass microscope slides. TUNEL FragEL DNA Fragmentation Detection Kit (Merck, Nottingham, UK) was used per manufacturer's instructions, except that proteinase K was omitted and replaced by 15 minutes in Triton X-100 0.1% in PBS. Immunohistochemistry was performed using primary antibodies to ED1 (1/400, monoclonal; ABD Serotec, Kidlington, UK) and OX42 (1/400, monoclonal; ABD Serotec; and 1/100, polyclonal; Santa Cruz Biotechnology, Inc., Heidelberg, Germany) with Texas red anti-mouse and Alexa Fluor 488 anti-rabbit IgG (both 1/400; Invitrogen, Grand Island, NY) secondary antibodies.

Retinal Whole Mounts and Counting of Photoreceptors

Anterior segments and vitreous were removed; eye cups were fixed in 4% PFA in PBS, and the neuroretina was dissected from the RPE except when it was adherent, in which case the RPE was dissected from the choroid. Retinae were permeabilized in 0.1% Triton X-100/4′,6-diamidino-2-phenylindole (DAPI) in PBS for 2 hours and mounted with DAPI mountant for cell counting. Images were captured at 63× magnification using a confocal laser scanning microscope (Zeiss, Hertfordshire, UK) running the LSM 510 software version 3.2 (Zeiss). Images were captured from three different areas (at 1/6, 3/6, and 5/6 of the radius) of each quadrant (total = 12 counts per eye) in the middle of the outer nuclear layer, to account for variation of photoreceptor

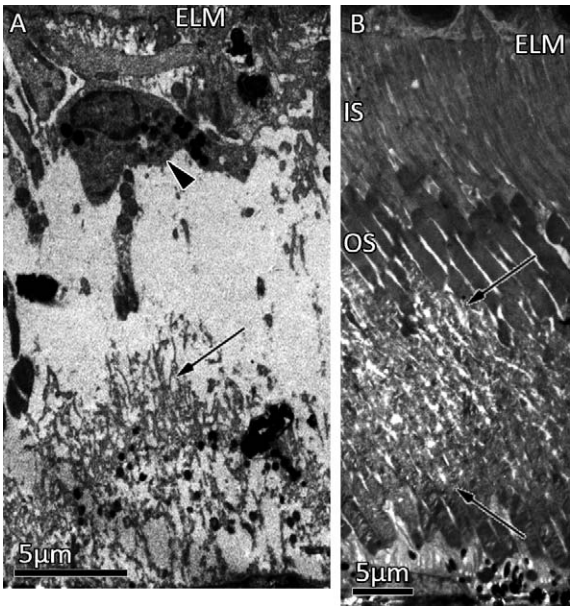

Figure 1. Electron micrographs of rat outer retina. (**A**) Two days after 22.6 g (0.6 J) weight drop to lateral sclera; absent photoreceptor inner segments (IS) and outer segments (OS) with RPE response (*arrowed*), disrupted external limiting membrane (ELM), and a macrophage (*arrowhead*). (**B**) Immediately after 31.3 g (0.6 J) weight drop to lateral sclera. Disrupted photoreceptor outer segments (OS; *arrowed above* and *below*).

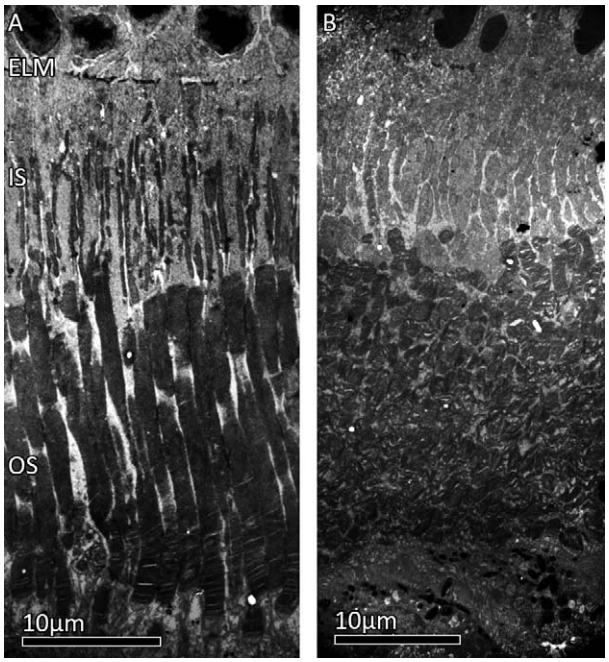

Figure 2. Electron micrographs of rat outer retina. (**A**) Normal control retina. (**B**) Disrupted photoreceptor inner (IS) and outer segments (OS) and external limiting membrane (ELM) 2 hours after ballistic injury.

numbers in the different areas, and quantified using the built-in particle counting facilities in ImagePro (Media Cybernetics, Bethesda, MD). Mean photoreceptor density per high-power field (0.146×0.146 mm) was expressed as a percentage of the mean value for uninjured control tissue.

Semithin (1 μm) toludine blue–stained retinal sections were cut 2 weeks after injury from the optic disc to the ciliary body through the center of the impact site; control tissue was taken from the (uninjured) inferior retina of animals killed at 2 hours after impact to the lateral sclera. Images were captured at 40× magnification (0.25×0.3 mm field of view) from five different areas of each section and quantified by a blinded observer using the user-defined manual counting facility in ImagePro. For display, counts were normalized as percentages of the mean value for uninjured control tissue in the same retinal area.

Statistical Analysis

Cell count and ERG data were normally distributed and analyzed with parametric tests in SPSS 19 (IBM, Armonk, NY). Means ± standard error were calculated for all samples. Electrophysiological data were analyzed using either three-way (time, intensity, injury) repeated measures ANOVA or generalized estimating equations for sets missing data (type III sum of squares). Nonsignificant interactions were removed from the models, and normality was assessed using residual plots.

Results

Weight Drop Did Not Create a Reproducible Retinal Injury

Two hours after impact to the central cornea, no injury was seen by clinical examination or light or electron microscopy. After direct scleral impact, retinal pathology was clinically occult, as the clinical examination and macroscopic appearances were normal. Photoreceptor outer segment disruption was induced in two of nine eyes to which 0.6 J was delivered; and, at this energy level, globe rupture occurred in two of nine eyes (Fig. 1).

Ballistic Trauma Created a Reproducible Retinal Injury

In cadaveric studies, a chamber pressure of $\geq$0.15 bar caused rupture in >50% of eyes. Weights of 0.91, 0.50, 0.16 (air gun pellets), and 0.095 g (ball bearing) were tested; 0.095 g was chosen to give the highest-velocity injury, 20 m/s at chamber pressure of 0.125 bar.

Immediately after injury, there was retinal pallor underlying the injury site in all eyes and variable vitreous hemorrhage. The pallor resolved over the next 2 weeks to leave an area of retinal atrophy revealing the choroidal vasculature.

Light and electron microscopy of resin-embedded retinal sections at 2 hours after injury showed disruption of photoreceptor outer and inner segments in all eight eyes and disruption of the external limiting membrane (ELM) in three eyes (Fig. 2).

Specific Photoreceptor Death Developed after Ballistic Blunt Ocular Trauma

By 2 weeks after ballistic injury, a large area of retinal and RPE atrophy developed. There was progressive loss of the ONL approaching the center of the impact site but relative preservation of the inner nuclear and ganglion cell layers, with hypopigmentation and irregularity of the underlying RPE (Figs. 3A, 3B). At the center of the impact site, all neuroretinal layers were absent.

The proportion of photoreceptors surviving increased at increasing distances from the center of the impact site, demonstrated by ONL cell counts on toludine blue–stained resin sections of the retina radially from the optic disc to the ciliary body, through the center of the lesion site (Fig. 3C).

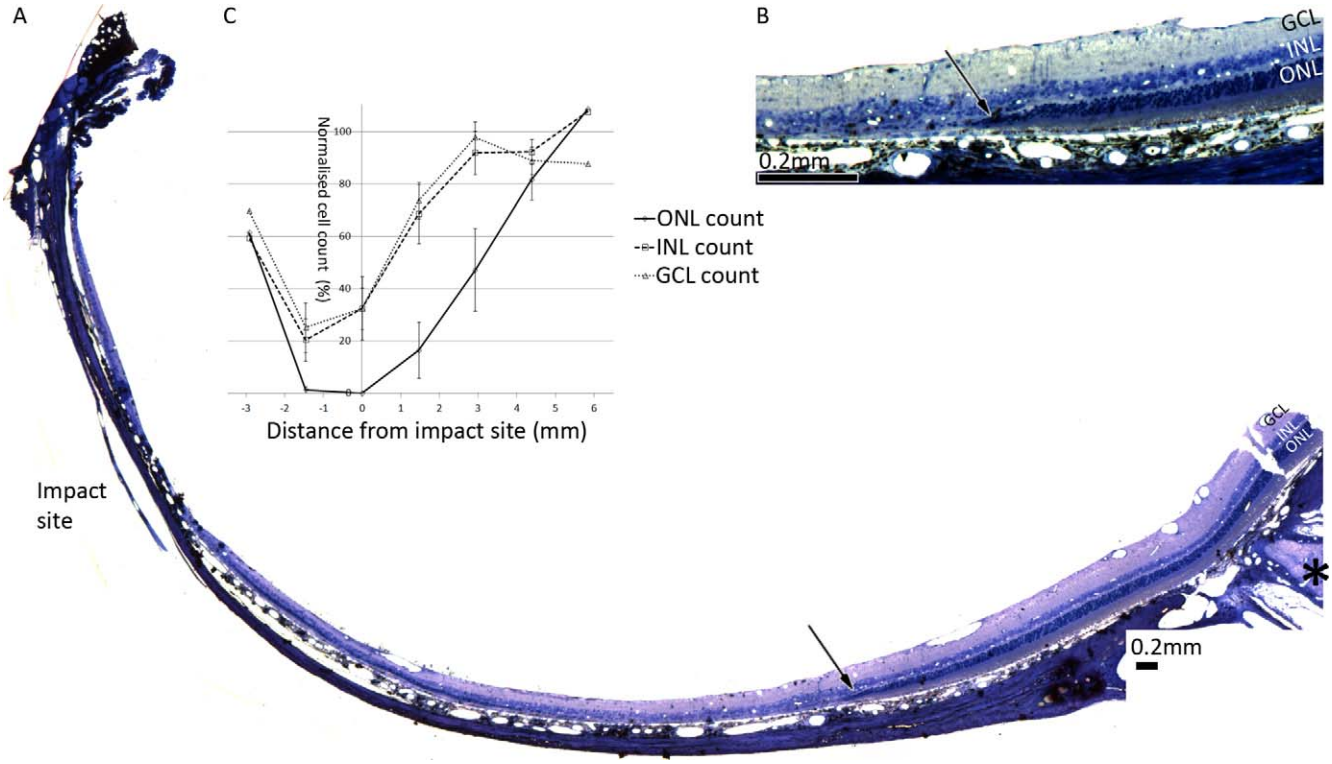

Figure 3. Light micrograph of rat retina 2 weeks after ballistic injury. (**A**) Outer nuclear layer (ONL) around the optic disc (*asterisk*) is normal. Approaching the impact site it thins (*arrowed*) and then disappears, leaving the inner retina relatively intact. (**B**) Line graph showing normalized retinal cell counts at distance from the impact site ± standard error of the mean. ONL survival is lowest, with the inner nuclear layer (INL) and ganglion cell layer (GCL) relatively spared. (**C**) Higher-power cutout of (**A**) showing thinning and loss of the ONL.

ONL cell counting on retinal whole mounts confirmed that 18.4 ± 4.6% of photoreceptors had died.

Photoreceptors Died by Necrosis and Apoptosis

By 2 hours after injury, there were occasional apoptotic nuclei in the ONL with chromatin condensation and nuclear blebbing (Fig. 4A). Two days after injury, in the center of the impact site, there was infiltration of macrophages (histiocytic, ED1-positive, OX42-negative; Figs. 4B, 4I–K, Supplementary Material and Supplementary Figs. S1C–H, http://www.iovs.org/lookup/suppl/doi:10.1167/iovs.12-9887/-/DCSupplemental),[20] edema, and necrotic nuclei in the ONL (Figs. 4B–E). In the perilesional area there was disruption of outer segments with inflammatory cell infiltration. There were fewer necrotic photoreceptor nuclei at increasing distances from the lesion site but more apoptotic photoreceptor nuclei (Figs. 4E–H; see Supplementary Material and Supplementary Figs. S1A, S1B http://www.iovs.org/lookup/suppl/doi:10.1167/iovs.12-9887/-/DCSupplemental). Centrally in the impact site, many cells with diffuse nuclear and cytoplasmic TUNEL staining were observed (Fig. 4L), probably because direct cellular injury caused necrotic death.[21] However, in areas away from the impact site, the presence of specific TUNEL-positive photoreceptor cell nuclei confirmed apoptosis of these cells (Figs. 4L–O).

Electrophysiological Assessment of Ballistic Injury

To assess retinal function, scotopic and photopic flash ERG series were recorded and the major components (a- and b-waves) observed. The a- and b-wave amplitudes were quantified and compared between injured and control eyes at 2, 7, and 14 days postinjury. The magnitude and latency of all components were intensity dependent, though only amplitude was injury dependent. ANOVA was used to compare scotopic (dark adapted) a-wave amplitudes. Scotopic a-wave amplitude was significantly reduced by injury (Fig. 5A; 1 *df*, $F = 59.7$, $P < 0.001$, $\eta = 0.895$), and there was no significant change between the three time points (2 *df*, $F = 2.706$, $P = 0.129$, $\eta = 0.279$). Since b-wave onset can obscure the a-wave, gradient of the a-wave's linear portion (leading edge) was measured, giving a trend similar to that observed for amplitude (1 *df*, $F = 40.9$, $P < 0.001$, $\eta = 0.854$). Scotopic b-wave amplitude was significantly reduced by injury (2 *df*, $F = 39.9$, $P < 0.001$, $\eta = 0.851$), though there was no significant effect on the scotopic b-/a-wave ratio (see Supplementary Material and Supplementary Fig. S2, http://www.iovs.org/lookup/suppl/doi:10.1167/iovs.12-9887/-/DCSupplemental; 1 *df*, $F = 4.917$, $P = 0.062$, $\eta = 0.413$). Photopic a-waves were frequently undetectable in injured and control eyes, and some data points were missing. Generalized estimating equations were therefore used to analyze photopic b-wave amplitudes, which were significantly reduced by injury (Fig. 5B; unstructured correlation matrix, 1 *df*, $P < 0.001$), consistent with the outer retinal injury affecting both cones and rods equally.

Discussion

This is the first murine model of closed globe injury to show that low-velocity ballistic trauma creates reproducible commotio retinae, with pathological features that mirror the clinical and OCT findings in humans after severe blunt ocular trauma.[17] At the impact site, there was necrosis of photoreceptors, and centrally there was death of all retinal cells

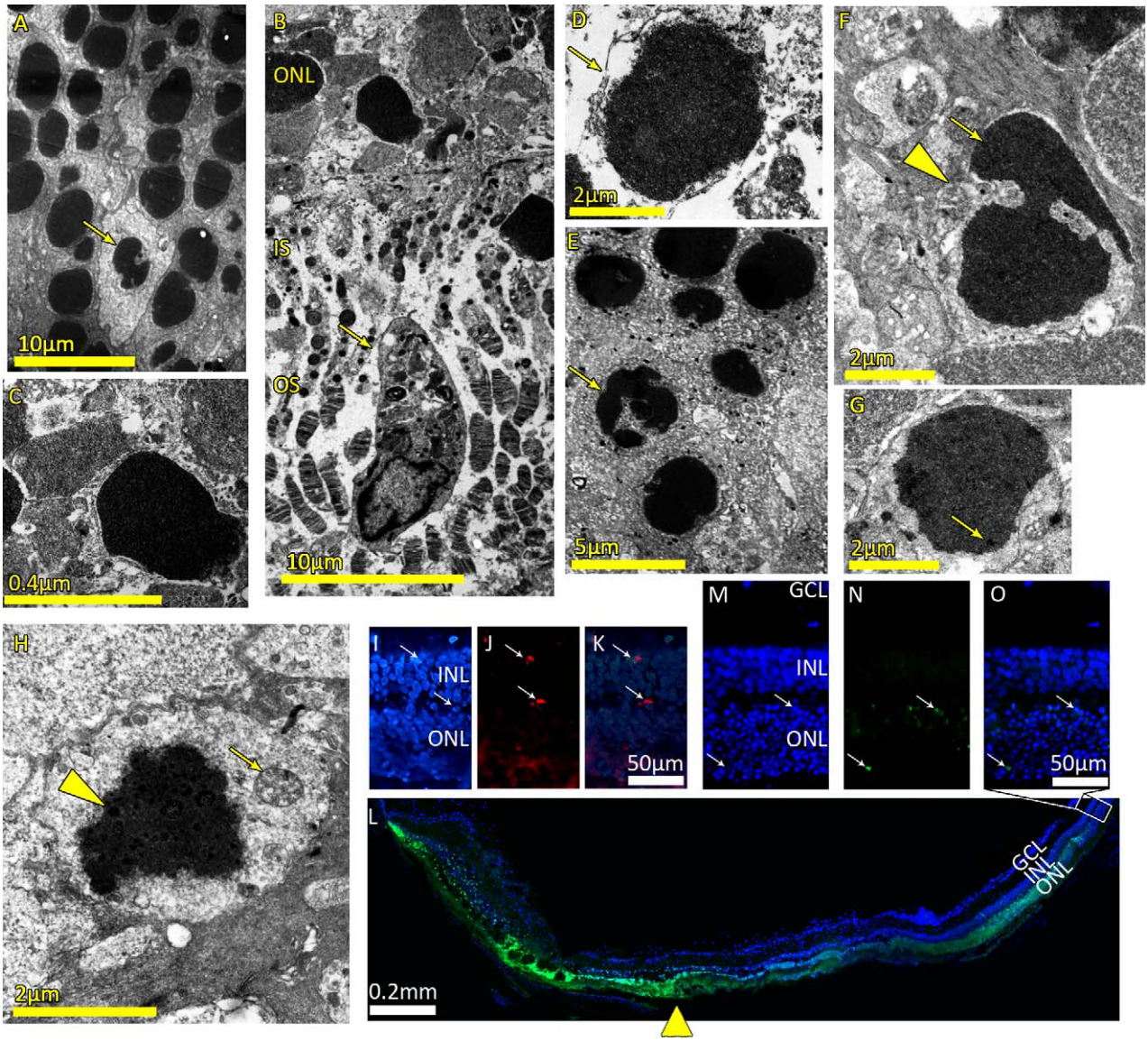

Figure 4. (**A–G**) Electron micrographs of rat outer retina. (**A**) Outer nuclear layer (ONL) 2 hours after ballistic injury; blebbed (apoptotic) photoreceptor nucleus *arrowed*. (**B–G**) Two days after ballistic injury. (**B**) Close to the impact site, macrophage removing disrupted photoreceptor outer and inner segments (*arrowed*) and nonspecific cell death with condensed and fragmented photoreceptor nuclei in the ONL, shown at higher magnification in (**C**). (**D**) Close to the impact site, necrotic photoreceptor nucleus in an edematous ONL with ruptured cell membranes (*arrowed*). (**E–H**) Apoptotic photoreceptor nuclei farther away from the impact site. (**E**) Nuclear blebbing (*arrowed*); (**F**) nuclear blebbing (*arrowed*) with invasion of the photoreceptor cytoplasm by Müller cell processes (*arrowhead*); (**G**) a condensed photoreceptor nucleus with chromatin condensation at the periphery of the nucleus, typical of apoptosis; (**H**) chromatin aggregates (*arrowhead*) dispersed throughout the condensed photoreceptor nucleus (rather than peripherally), but the intact mitochodrion (*arrowed*) is suggestive of apoptosis. (**I–K**) ED1 staining showing DAPI-stained nuclei (**I**), *red* ED1-positive macrophages (*arrowed*) in the inner nuclear layer (INL) and ONL (**J**), and combined image (**K**). (**L**) TUNEL staining. The frequency of TUNEL-positive cells is highest in the ONL centrally to the impact site (*arrowhead*), reducing in frequency with increasing distance. (**M–O**) High-power cutout of (**L**): DAPI-stained nuclei (**M**), apoptotic photoreceptor nuclei (*arrowed*, **N**), combined image (**O**).

(sclopetaria retinae). Away from the impact site, photoreceptor death occurred by a combination of apoptosis and necrosis. Preservation of the inner retinal layers, together with specific photoreceptor cell death, mirrored human OCT findings. The reason this injury predominantly affects photoreceptors is unclear, but we suggest that shearing forces at the neuroretina–RPE junction during globe deformation make them particularly vulnerable.

The spectrum of cell death ranges between apoptosis and necrosis, with significant overlap. We have shown cells that are clearly necrotic (Figs. 4C, 4D) and cells that exhibit features consistent with apoptosis (Figs. 4E–H, 4L–O; see Supplementary Material and Supplementary Figs. S1A, S1B, http://www.iovs.org/lookup/suppl/doi:10.1167/iovs.12-9887/-/DCSupplemental), though it is likely that many photoreceptors undergo a mixed form of cell death. While necrosis is an unregulated form of cell death, apoptosis is mediated by specific cell death signaling pathways, as is the mixed form of cell death, termed necroptosis, and these pathways can be modulated to increase cell survival.[18,22] Thus, our results imply that in a proportion of photoreceptors after ballistic retinal injury, cell death is mediated by apoptotic or necroptotic

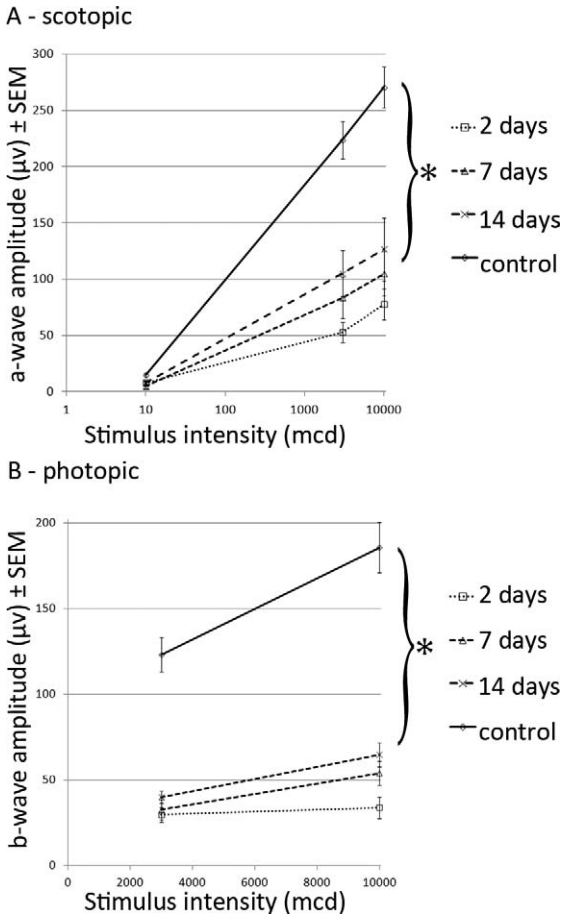

Figure 5. Quantification of the relevant components of the ERG at 2, 7, and 14 days after injury displayed as amplitude ± standard error of the mean (SEM) at increasing stimulus intensity. (**A**) Scotopic (dark adapted) a-wave amplitude was significantly reduced by injury at all time points and stimulus intensities (*$P < 0.001$), and (**B**) photopic (light adapted) b-wave amplitude was similarly reduced.

regulated signaling pathways, with a potential for successful neuroprotective therapies.

In human studies, mild commotio retinae associated with photoreceptor recovery is characterized by outer segment disruption, whereas severe commotio retinae is associated with photoreceptor inner and outer segment disruption observed by OCT.[17] Inner segment disruption was also present in our model, but has not been reported in other (mild, recovering) animal models of commotio retinae. The RPE and photoreceptor outer and inner segments appear as three bands on spectral-domain OCT. The thinner line above them may represent the ELM or the myoid portion of the cone inner segments.[23] Loss of this line on OCT may be a marker of severe photoreceptor damage in commotio retinae and age-related macular degeneration.[17,24] If it represents cone inner segments, we speculate that disruption of these mitochondria-rich structures (seen in our model) is a lethal injury to photoreceptors, while outer segment disruption is less likely to cause photoreceptor death.

In our hands, the severity of weight drop–induced retinal injuries was inconsistent in rats. The energy threshold for inducing commotio retinae is close to that causing rupture (approximately 0.6 J). That low-velocity injury does not usually cause commotio retinae is consistent with the body of literature on commotio retinae induced by high-velocity impact.[12] In contrast, a lower-energy injury with a 0.095 g pellet traveling at 20 m/s (0.019 J) reproducibly created central sclopetaria retinae at the impact site and surrounding commotio retinae. High-velocity impact of a low-weight projectile creates more injury than low-velocity impact by a heavy projectile, despite similar kinetic energies[25]; and the curved profile of ball bearings used for ballistic trauma in this study resulted in a higher area-normalized impact energy (lower with a larger projectile), which is a better predictor of corneoscleral stress and vitreous pressure than impact energy alone.[26] The ultrastructural features of our ballistic retinal injury model are consistent with other studies of commotio retinae, showing disruption of photoreceptor outer segments.

The rat lens accounts for 60% of axial length.[27] With such a small vitreous cavity, it is likely that the lens impacted the retina during injury in our experiments with potential crushing of the retina. This is also the case in larger animals in which ocular dimensions are similar to those in humans,[12] though with the larger lens this crushing will be more extensive in the rat.

The a-wave is the initial negative deflection caused by photoreceptor activation (rods in scotopic series, cones in photopic series) and is routinely used to measure photoreceptor function. The b-wave is the first positive deflection, immediately following the a-wave, and is generated by the activity of second-order neurons (such as ON bipolar cells in the inner nuclear layer). The b-wave is therefore dependent on photoreceptor activation and synaptic transmission in addition to inner retinal function. The ERG in the injured eyes showed a significant reduction in a- and b-wave amplitude compared to the control eyes without any change in implicit time. The b-/a-wave ratio is a measure of how much of the variation in b-wave amplitude is explained by variation in the magnitude of photoreceptor activation compared to the function of second-order neurons; this ratio was normal and similar between injured and control eyes. These reductions in ERG amplitude occurred under both scotopic and photopic conditions and would be consistent with damage primarily to the photoreceptor layer.

Rods make up 99% of rat photoreceptors[28] and, in our model, scotopic a-wave amplitude (which reflects rod function) was reduced by >50% (Fig. 5), although only 18% of photoreceptors died. The degree of ERG reduction was therefore disproportionate to the amount of histological photoreceptor death. Either outer segment damage or photoreceptor remodeling (similar to that seen after retinal detachment[29]) could reduce the a-wave. Additionally, the photoreceptor component (leading edge) of the a-wave is sensitive to extracellular Ca^{2+} and K^{+} levels,[30] which may be affected either by altered Müller glial function or by local structural changes.

In conclusion, we report an animal model of the outer retinal changes that occur after severe commotio retinae in humans, which is the first murine rodent model of blunt ocular trauma. Our results suggest that outer retinal atrophy occurs as a result of photoreceptor apoptosis and necrosis due to a terminal injury to photoreceptor inner segments. The observed photoreceptor apoptosis is translationally relevant because there is the potential to prevent neuronal death and improve visual outcomes with use of antiapoptotic neuroprotective therapies. This model provides an opportunity for both mechanistic and translational therapeutic studies.

Acknowledgments

We thank Peter Nightingale (Queen Elizabeth Hospital, Birmingham, UK) for statistical advice and Theresa Morris and Katharine Griffiths (University of Birmingham) for technical support.

References

1. Wong TY, Klein BE, Klein R. The prevalence and 5-year incidence of ocular trauma. The Beaver Dam Eye Study. *Ophthalmol*. 2000;107:2196–2202.
2. Jones NP, Hayward JM, Khaw PT, Claoue CM, Elkington AR. Function of an ophthalmic "accident and emergency" department: results of a six month survey. *Br Med J*. 1986; 292:188–190.
3. Vernon SA. Analysis of all new cases seen in a busy regional centre ophthalmic casualty department during 24-week period. *J R Soc Med*. 1983;76:279–282.
4. Blanch RJ, Scott R. Military ocular injury: Presentation, assessment and management. *J R Army Med Corps*. 2010; 155:279–284.
5. Weichel ED, Colyer MH, Ludlow SE, Bower KS, Eiseman AS. Combat ocular trauma visual outcomes during operations Iraqi and Enduring Freedom. *Ophthalmol*. 2008;115:2235–2245.
6. Pieramici DJ, Sternberg P Jr, Aaberg TM Sr, et al. A system for classifying mechanical injuries of the eye (globe). The Ocular Trauma Classification Group. *Am J Ophthalmol*. 1997;123: 820–831.
7. Chalioulias K, Sim KT, Scott R. Retinal sequelae of primary ocular blast injuries. *J R Army Med Corps*. 2007;153:124–125.
8. Berlin R. Zur sogenannten commotio retinae. *Klin Monatsbl Augenheilkd*. 1873;1:42–78.
9. Hart JC, Natsikos VE, Raistrick ER, Doran RM. Chorioretinitis sclopetaria. *Trans Ophthalmol Soc U K*. 1980;100:276–281.
10. Eagling EM. Ocular damage after blunt trauma to the eye. Its relationship to the nature of the injury. *Br J Ophthalmol*. 1974;58:126–140.
11. Saleh M, Letsch J, Bourcier T, Munsch C, Speeg-Schatz C, Gaucher D. Long-term outcomes of acute traumatic maculopathy. *Retina*. 2011;31:2037–2043.
12. Blanch RJ, Ahmed Z, Berry M, Scott RAH, Logan A. Animal models of retinal injury. *Invest Ophthalmol Vis Sci*. 2012;53: 2913–2920.
13. Hart JC, Blight R, Cooper R, Papakostopoulos D. Electrophysiological and pathological investigation of concussional injury. An experimental study. *Trans Ophthalmol Soc U K*. 1975;95: 326–334.
14. Sipperley JO, Quigley HA, Gass JD. Traumatic retinopathy in primates: the explanation of commotio retinae. *Arch Ophthalmol*. 1978;96:2267–2273.
15. Liem AT, Keunen JE, van Norren D. Reversible cone photoreceptor injury in commotio retinae of the macula. *Retina*. 1995;15:58–61.
16. An MX, Zhang XF, Zhang JS. Oxidative damage and photoreceptor cell apoptosis in contusion injury of the rabbit retina [in Chinese]. *Zhonghua yan ke za zhi [Chin J Ophthalmol]*. 2004;40:118–121.
17. Souza-Santos F, Lavinsky D, Moraes NS, Castro AR, Cardillo JA, Farah ME. Spectral-domain optical coherence tomography in patients with commotio retinae. *Retina*. 2011;32:711–718.
18. Ahmed Z, Kalinski H, Berry M, et al. Ocular neuroprotection by siRNA targeting caspase-2. *Cell Death Dis*. 2011;2:e173.
19. Courtney M, Edwards B. Measuring bullet velocity with a PC soundcard. ArXiv preprint physics/0601102. 2006.
20. Streit WJ. Microglia. In Kettenmann H, Ransom BR, eds. *Neuroglia*. 2nd ed. New York, NY: Oxford University Press; 2005:63.
21. van Lookeren Campagne M, Gill R. Ultrastructural morphological changes are not characteristic of apoptotic cell death following focal cerebral ischaemia in the rat. *Neurosci Lett*. 1996;213:111–114.
22. Trichonas G, Murakami Y, Thanos A, et al. Receptor interacting protein kinases mediate retinal detachment-induced photoreceptor necrosis and compensate for inhibition of apoptosis. *Proc Natl Acad Sci U S A*. 2010;107:21695–21700.
23. Gloesmann M, Hermann B, Schubert C, Sattmann H, Ahnelt PK, Drexler W. Histologic correlation of pig retina radial stratification with ultrahigh-resolution optical coherence tomography. *Invest Ophthalmol Vis Sci*. 2003;44:1696–1703.
24. Oishi A, Hata M, Shimozono M, Mandai M, Nishida A, Kurimoto Y. The significance of external limiting membrane status for visual acuity in age-related macular degeneration. *Am J Ophthalmol*. 2010;150:27–32.e1.
25. Scott WR, Lloyd WC, Benedict JV, Meredith R. Ocular injuries due to projectile impacts. *Annu Proc Assoc Adv Automot Med*. 2000;44:205–217.
26. Weaver AA, Kennedy EA, Duma SM, Stitzel JD. Evaluation of different projectiles in matched experimental eye impact simulations. *J Biomech Eng*. 2011;133:031002.
27. Hughes A. A schematic eye for the rat. *Vision Res*. 1979;19: 569–588.
28. Szel A, Rohlich P. Two cone types of rat retina detected by anti-visual pigment antibodies. *Exp Eye Res*. 1992;55:47–52.
29. Fisher SK, Lewis GP, Linberg KA, Verardo MR. Cellular remodeling in mammalian retina: results from studies of experimental retinal detachment. *Prog Retin Eye Res*. 2005; 24:395–431.
30. Vinberg FJ, Strandman S, Koskelainen A. Origin of the fast negative ERG component from isolated aspartate-treated mouse retina. *J Vis*. 2009;9:9.1–17.